

# Sorting Cells by Size, Shape and Deformability

Jason P. Beech, Stefan H. Holm, Karl Adolfsson and Jonas O. Tegenfeldt

## Electronic Supporting Information

### 1 Materials and methods

#### 1.1 Device design

Our devices were designed with 13 sections, each with one  $R_c$  as shown in Fig. ESI 1 using the equation in Fig. ESI 1I. The diameter of the posts,  $D_{\text{post}} = 20\text{ }\mu\text{m}$  and the gap between the posts,  $d = \lambda - D_{\text{post}} = 12\text{ }\mu\text{m}$  throughout the device ( $\lambda$  is the centre-to-centre spacing of the posts).  $R_c$  is varied in the device by varying  $\Delta\lambda$ , the amount each row is laterally shifted with regard to the previous row as shown in Figure ESI 1F. The small deviations from whole and half micrometer values for  $R_c$  are the result of having to fit to the  $0.2\text{ }\mu\text{m}$  manufacturing grid used in the mask generating process.

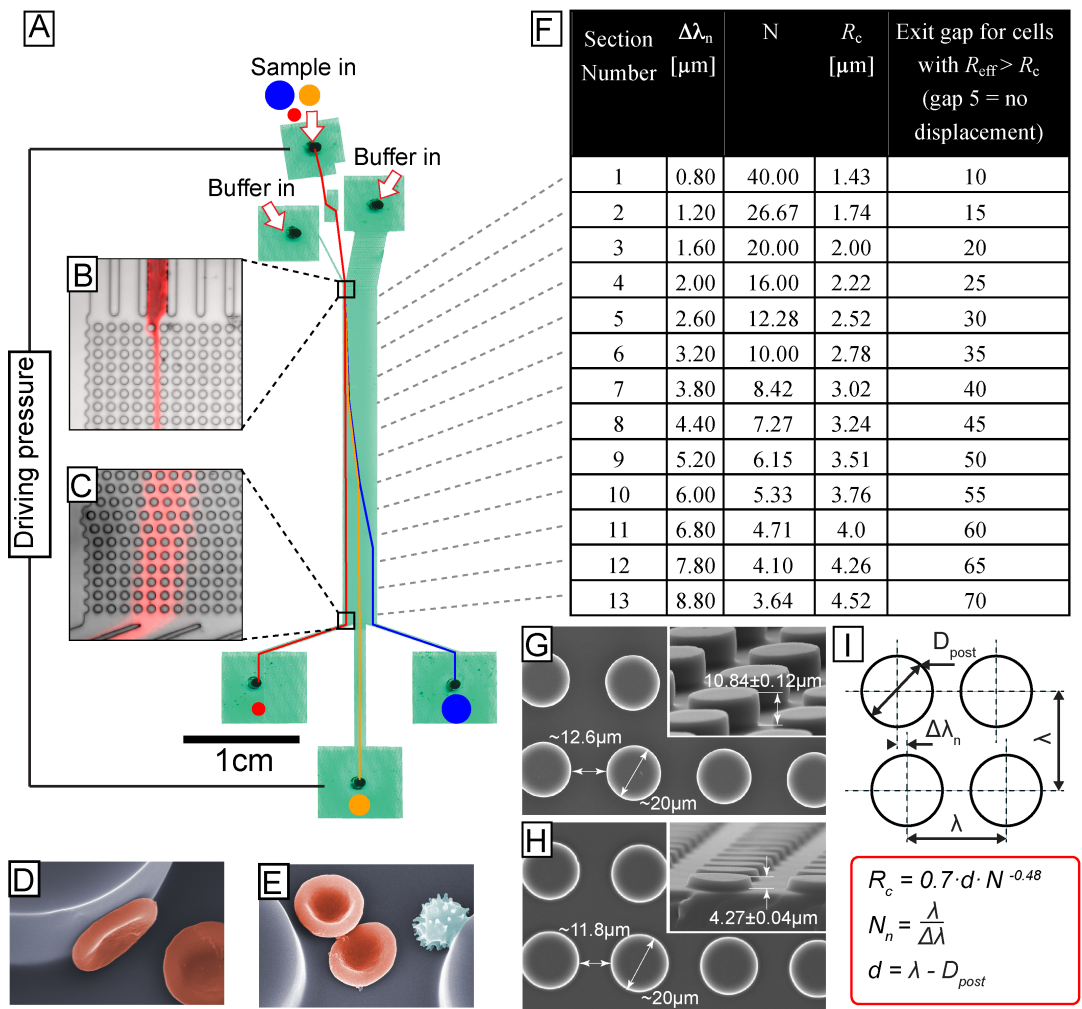


Fig. ESI 1 Overview of our device design. (A) To make an overview image of the device it is filled with green food colour and imaged by scanning in a flat-bed scanner. Sample is injected in the central channel and focused with a flow of buffer from the sides by controlling the over-pressure in the three inlets (outlets are kept at ambient pressure). The larger the particles are, the more they are displaced to the right as illustrated by the coloured lines. (B) A colour enhanced micrograph showing red blood cells being injected into the device. (C) In this device ( $10.8\text{ }\mu\text{m}$  deep) normal, disc-shaped red blood cells are not displaced. (D) and (E) False-coloured SEM images illustrating the dimensions of RBCs in relation to the dimensions of the two devices used, which are shown in (G) and (H). The red cells are normal discocytes and the blue cell is an echinocyte. (F) The devices contain posts with a diameter of  $20\text{ }\mu\text{m}$  and gaps of  $12\text{ }\mu\text{m}$  throughout. 13 sections with different critical radii  $R_c$  are achieved by varying the period  $N$  as shown in the table.  $R_c$  is calculated using the equation shown in (I).

Cells are injected into the device between posts 5 and 6 (counted from the left wall, see Fig. ESI 1 B below) which we denote gap 5. For each section, where the effective size of the cell is larger than the critical size the total displacement from the wall is increased by 5 gaps. Cells with an effective radius between  $2.0\ \mu\text{m}$  and  $2.22\ \mu\text{m}$  for example will be displaced in sections 1, 2 and 3 but not in section 4. The resulting displacement will be  $5 + 5 + 5 = 15$  gaps. Being injected at gap 5 and then displaced by 15 gaps means that these cells are “binned” together and will leave the device through gap 20. In reality though, imperfections in the device and the fluid flow, the random nature of diffusion, rotation and cell-cells interactions together with a finite dispersion in the size of a given cell type smooth out the outlet distributions, as can be seen in Fig. 2 in the main body of the paper.

## 1.2 Device fabrication

To make masters for replica moulding SU-8 (MicroChem, Newton, MA, USA) was spin coated onto 3" silicon wafers at thicknesses of  $4.27 \pm 0.04\ \mu\text{m}$  and  $10.84 \pm 0.12\ \mu\text{m}$  and patterned using UV light in a contact mask aligner (Karl Suss MJB3 and MJB4, Munich, Germany). A chrome mask was fabricated by Delta Mask (Delta Mask, Enschede, The Netherlands) with a design drawn in L-Edit 11.02 (Tanner Research, Monrovia, CA USA). An anti-adhesion layer of 1H,1H,2H,2H-perfluorooctyltrichlorosilane (ABCR GmbH & Co. KG, Karlsruhe, Germany) was applied before casting to facilitate demoulding. PDMS monomer and hardener (Sylgard 184, Dow Corning, Midland, MI, USA) were mixed to a ratio of 10:1, degassed, poured onto the master and baked for 1 hour at  $80\ ^\circ\text{C}$ . Holes were punched in the patterned PDMS slab for fluidic connections and the slab was then bonded to a blank, PDMS-covered microscope slide following surface treatment with oxygen plasma (Plasma Preen II-862, Plasmatic Systems, Inc, North Brunswick, NJ, USA) to achieve a sealed device. Connection tubes were attached using a silicone adhesive (A07, Wacker Chemie AG, München, Germany).

## 1.3 Surface treatment

As a compliment to autoMACS<sup>TM</sup> buffer, which contains EDTA as an anticoagulant and BSA to prevent the adhesion of proteins to surfaces, the adhesion of blood cells to the inner surfaces of our devices was further decreased by formation on the PDMS of a polymer brush. Immediately after  $\text{O}_2$  plasma treatment and bonding, devices were filled with 0.2% PLL(20)-g[3.5]-PEG(2) (SuSoS AG, Dübendorf, Switzerland) in DI water and allowed to rest for at least 20 min before rinsing with autoMACS<sup>TM</sup> running buffer prior to running an experiment.

## 1.4 Red blood cell morphology and deformability changing protocols

Blood was extracted from healthy volunteers via finger pricking and diluted around 5 times in autoMACS<sup>TM</sup> running buffer (Miltenyi Biotech, Auburn, CA). Blood cell morphologies were altered by the addition of sodium salicylate to 2 mM (to form echinocytes) or Triton X-100 to 0.06% (to form stomatocytes) to the autoMACS<sup>TM</sup> prior to the addition of blood. Deformability of echinocytes was altered by fixation with 0.003% glutaraldehyde.

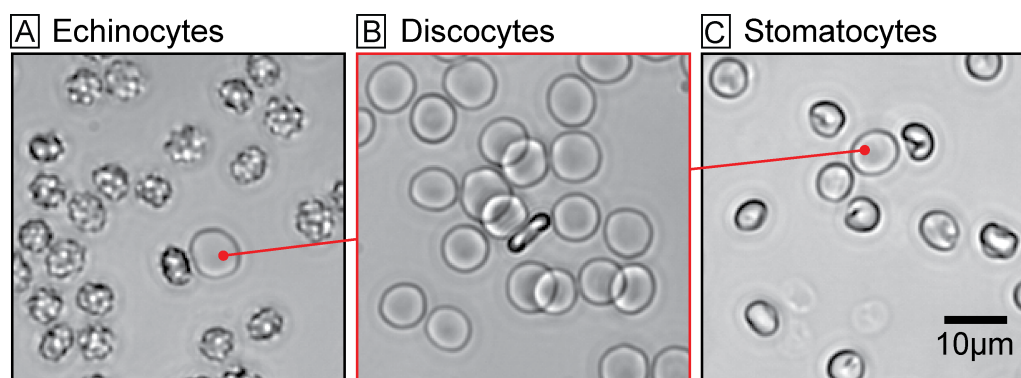


Fig. ESI 2 Transmission microscopy images of red blood cells with different morphologies. (A) Echinocytes formed using 16mM Sodium Salicylate. (B) Normal discocytes in autoMACS<sup>TM</sup> buffer. (C) Stomatocytes formed using 577 ppm Triton X-100. With both the Sodium Salicylate and Triton X-100 ~1% of RBCs retain a discocytic shape.

#### 1.4.1 Sodium salicylate to form echinocytes

To 100  $\mu$ l of autoMACS<sup>TM</sup> buffer is added 7  $\mu$ l of 0.3 M Sodium Salicylate and this in turn is added to 20  $\mu$ l of freshly drawn blood. The running buffer is 200  $\mu$ l of autoMACS<sup>TM</sup> buffer with 14  $\mu$ l 0.3 M Sodium Salicylate.

Final concentrations: autoMACS<sup>TM</sup> = 79% Sodium Salicylate = 16 mM, Blood = ~16% of whole blood

Sodium salicylate (SS) is an aspirin derivative. It is known to incorporate into the outer leaflet of the RBC membrane and is therefore an echinocytic agent. Concentrations of SS significantly less than 2 mM lead to the formation of a population of echinocytes with a broad distribution in shapes including stomatocytes, discocytes and echinocytes<sup>1</sup>. It is believed that this spread in morphologies stems from the distribution in cell age, cytoskeletal differences and/or metabolic rate. As the concentration of SS is increased the mean shape of the populations is driven towards the echinocytic. At 2 mM 98% of RBCs have been shown to adopt echinocytic forms, with the remaining 2% keeping their discocytic shape<sup>1</sup>. Using a simple analysis of optical microscopy images like those shown in Fig. ESI 2 A, we found that of 1846 RBCs treated with SS, 1.1% retained a discocytic shape. An increase in cell stiffness accompanies the shape changes caused by SS<sup>1</sup>.

#### 1.4.2 Triton X-100 to form stomatocytes

To 100  $\mu$ l of autoMACS<sup>TM</sup> buffer is added 1.4  $\mu$ l of 5% Triton X-100 and this in turn is added to 20  $\mu$ l of freshly drawn blood. The running buffer is 200  $\mu$ l of autoMACS<sup>TM</sup> buffer with 0.8  $\mu$ l of 5% Triton X-100.

Final concentrations: autoMACS<sup>TM</sup> = 82%, Triton X-100 = 577ppm, Blood = ~16% of whole blood

The non-ionic surfactant Triton X-100 is known to be a potent stomatocytic agent. However, care must be taken when using Triton X-100 to induce stomatocytes as the surfactant is also a haemolytic agent. The ability of RBCs to change shape without being lysed depends on the buffer. We found that when using autoMACS<sup>TM</sup> (BSA and EDTA) as a buffer, a concentration of 0.06% Triton X-100 gave sufficiently well-formed stomatocytes that were stable over the time scales, ~1 hour, of our experiments. As with echinocytes, the population of stomatocytes formed is not completely homogeneous. Of 1372 RBCs treated with Triton X-100, 1.0% retained a discocytic shape, see Fig. ESI 2 C.

#### 1.4.3 Fixation of echinocytes in 0.003% glutaraldehyde

10  $\mu$ l of freshly drawn blood was added to 200  $\mu$ l cold PBS, the cells spun down at 600 g for 30 seconds and the supernatant replaced with 200  $\mu$ l of fresh PBS. This was repeated 3 times. On the fourth time the supernatant was exchanged for 200  $\mu$ l new PBS with 0.003% glutaraldehyde and the cells incubated at room temperature for 30 minutes. Finally the cells were spun down and the supernatant replaced with 100  $\mu$ l of cold autoMACS<sup>TM</sup> buffer.

*Note: The glutaraldehyde stock solution was 20% in methanol. While methanol might affect the morphology of the cells this was not apparent during either light or electron microscopy. The change in deformability due to the fixation with glutaraldehyde is also assumed to dominate any effects from the small amounts of methanol present.*

#### 1.4.4 SEM preparation

SEM images were taken on LEO 1560 (Carl Zeiss SMT GmbH, Oberkochen, Germany) after fixation with glutaraldehyde and metalisation with 10nm of platinum.

### 1.5 Running experiments

A pressure gradient was used to drive flow through the DLD devices. Outlets were kept at atmospheric pressure and the overpressure at the three inlets was controlled individually in the range 5-800 mbar using an MFCS-4C pressure controller (Fluigent, Paris, France). Pressure control at each of the three inlets made it possible to hydrodynamically focus the sample into a stream of ~10  $\mu$ m in width as can be seen in Fig. ESI 1B. The concentration of RBCs in the device is also controlled by flow focusing such that the distance between cells is kept larger than the distance the cells move between movie frames, a condition that facilitates particle tracking. When particle tracking is not required much higher concentrations can be used.

All images were taken through an inverted Nikon Eclipse TE2000-U microscope (Nikon Corporation, Tokyo, Japan). High speed images were taken using an EoSens mini MC-1370 camera (Mikrotron GmbH, Unterschleißheim, Germany). In all other cases an Andor Luca or Andor Ixon EMCCD camera (Andor Technology, Belfast, Northern Ireland) were used.

Fluorescent polystyrene microspheres with diameters of 3.00 $\pm$ 0.15  $\mu$ m, (Duke Scientific Corp. Palo-Alto, CA; R0300) and 4.87 $\pm$ 0.12  $\mu$ m (Polysciences Inc., Warrington, PA 18340), that are much less deformable than RBCs were used to evaluate the effects of particle deformation in our devices.

## 1.6 Analysis

Particle tracking software was written in MATLAB 2009b (The MathWorks, Natick, MA, USA). The tracking program was based on IDL Particle Tracking software, available at <http://www.physics.georgetown.edu/matlab/>). The tracking core was optimized for our specific setup. The software was able to track many particles in a field of view when the signal-to-noise ratio was sufficiently high and when the concentration was low enough to avoid particle overlap allowing measurement of the total displacement of hundreds of particles at the end of the device for each set of experimental conditions. White blood cells are either trapped at the inlets of our devices or are displaced to a greater extent than the RBCs allowing us to easily identify them. They do not interfere with our measurements and are not included in the particle counting.

## 2 Effects of device depth

Fig. ESI 3 shows discocytes in devices of different depths. Shear rates have been chosen such that deformation is kept to a minimum. As can also be seen in ESI Movies 1-7, in devices deeper than the diameter of the discocyte, the cells are able to rotate and it is half of the cell thickness ( $\sim 1.25 \mu\text{m}$ ) that defines  $R_{\text{eff}}$ . In devices shallower than the cell diameter, cells are unable to fully rotate and  $R_{\text{eff}}$  increases. In a device of  $3 \mu\text{m}$  depth the radius of the cell ( $\sim 3.75 \mu\text{m}$ ) defines  $R_{\text{eff}}$ . It is interesting that the discocytes do not fully rotate in the  $8 \mu\text{m}$  deep device. We believe that this is due to some coupling between the cell and the walls of the device although more investigations are required. It is also interesting to note that in devices of depths between the radius and half of the thickness of the discocyte the cell becomes tilted at an angle between  $0^\circ$  (lying in the plane of the device) and  $90^\circ$  (standing up against the post). This means that as shear rate is increased the strain, which is toward the surface of the post, will not only compress but also bend the cell. This could provide a means of measuring the bending modulus of cells or other particles.

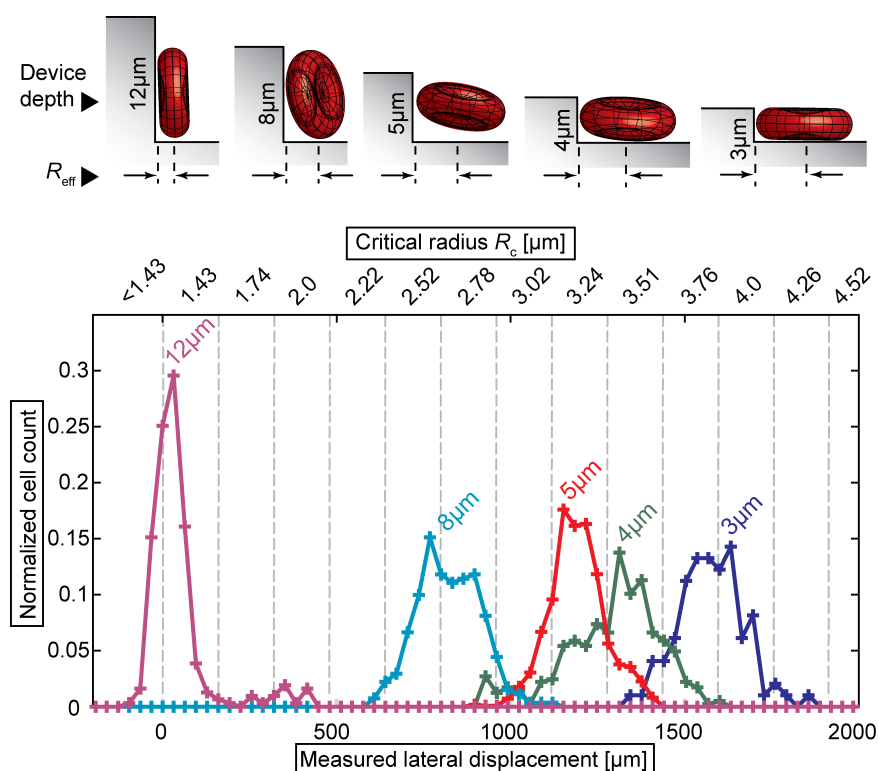


Fig. ESI 3 The effective size,  $R_{\text{eff}}$ , of non-spherical particles (discocytes) increases as device depth decreases. The device depth is shown next to each curve.



### 3 High-speed movies of RBC deformation

Movies of discocytes, echinocytes and stomatocytes in devices of 4.27  $\mu\text{m}$  and 10.84  $\mu\text{m}$  in depth representative of the typical behaviour of the cells. Colour enhanced still images from the movies are compiled in Fig. ESI 4.

ESI Movie1 – Discocyte in 4.3  $\mu\text{m}$  deep device + overview of inlet and outlet

ESI Movie2 – Discocyte in 10.8  $\mu\text{m}$  deep device

ESI Movie3 – Echinocyte in 4.3  $\mu\text{m}$  deep device

ESI Movie4 – Echinocyte in 10.8  $\mu\text{m}$  deep device

ESI Movie5 – Stomatocyte in 4.3  $\mu\text{m}$  deep device

ESI Movie6 – Stomatocyte in 10.8  $\mu\text{m}$  deep device

ESI Movie7 – Discocyte in 10.8  $\mu\text{m}$  deep device – cell rotates and thickness defines effective size

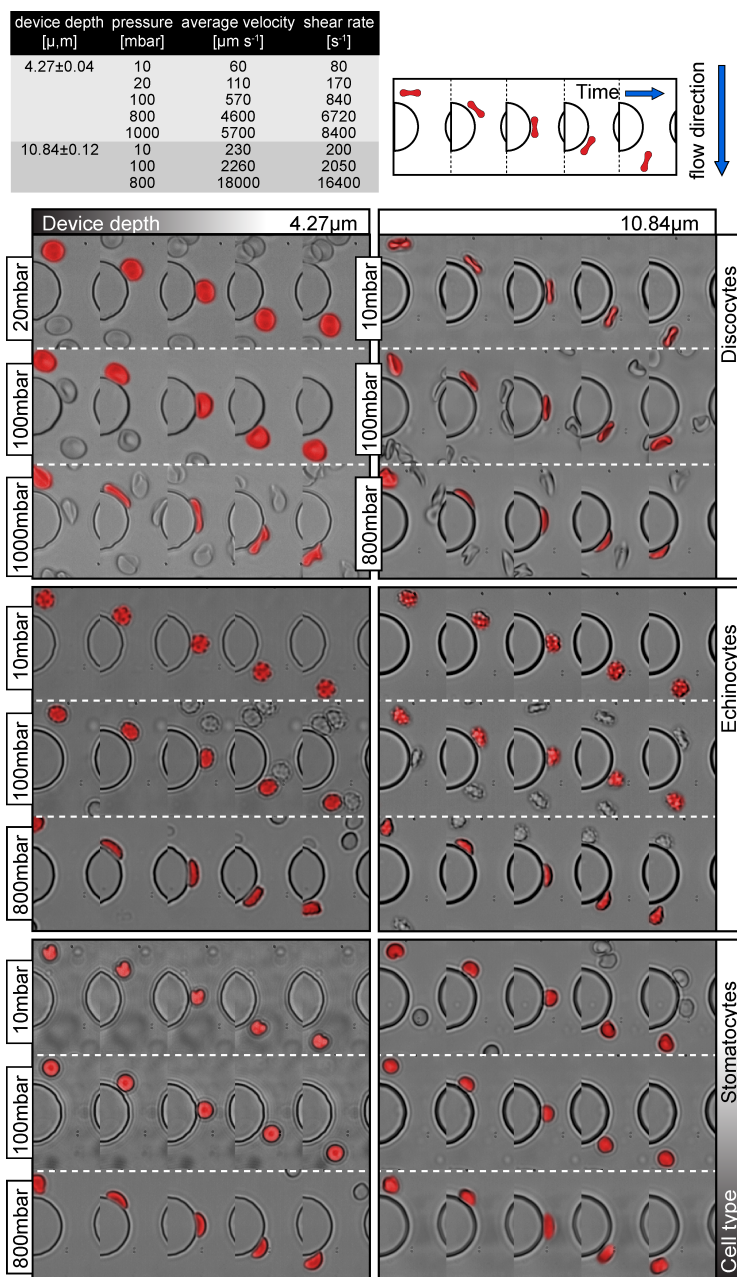


Fig. ESI 4 Colour-enhanced compilations of high-speed camera images, taken from movies 1-6, of cells moving through our devices. Each box shows one type of cell morphology in one of two devices (4.27 and 10.84  $\mu\text{m}$  deep) at three driving pressures. The insets at the top show, to the left, the average fluid flow velocity and wall shear rates at the pressures used, and on the right, how time evolves from left to right in the images. The effect of device depth on the orientation of discocytes can clearly be seen. Because echinocytes and stomatocytes are more spherical, their orientation due to device depth has less effect on their behaviour. At 10 mbar all cell types keep their morphologies but at higher pressures, in both devices, the cells are deformed and  $R_{\text{eff}}$  decreases.

#### 4 Decreasing deformability of echinocytes by fixation

Echinocytes were formed and subsequently fixated to decrease deformability using the protocols describes above. Fixation does not change the shape of the cells and, as can be seen in Fig. ESI 5, at shear rates below  $\sim 2050 \text{ s}^{-1}$  ( $\sim 10 \text{ mbar}$ ) the fixated echinocytes (right) and unfixated echinocytes (left) are not separated. However, the increased stiffness of the fixated cells gives them a considerably larger  $R_{\text{eff}}$  as shear rates are increased and at  $\sim 12300 \text{ s}^{-1}$  ( $\sim 300 \text{ mbar}$ ) separation is complete.

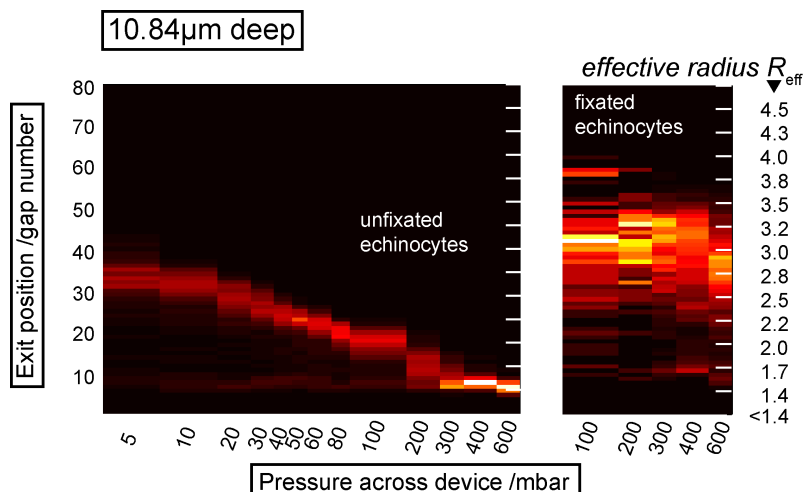


Fig. ESI 5 The stiffness of particles has a large effect on their trajectories through our devices. The effective size of echinocytes (left) decreases as they become deformed at high shear rates. Fixated echinocytes (right) are stiffer and are not deformed as readily, i.e. their effective size decreases less as the shear rate is increased. (At pressures below 100 mbar the fixated cells stick to the surface of the device and become trapped. This appears to be due to the fixation and is not a problem for normal, unfixated cells.)

#### 5 Is deformation responsible for the change in $R_{\text{eff}}$ ?

To exclude any other effects beyond deformation such as hydrodynamic lift that may be involved in decreasing  $R_{\text{eff}}$  we repeated the experiments with hard polystyrene spheres. Also, because PDMS is an elastomer, one would expect microfluidics channels fabricated in PDMS to deform to some degree under the pressures used to drive fluid flow. Hardy et al showed how the height of channels, initially  $500 \mu\text{m}$  wide and  $\sim 40 \mu\text{m}$  deep change due to this effect<sup>2</sup>. While Hardy's channels experienced changes in depth of as much as 20-30% in the pressure range we are using, our channels are filled with posts at  $\sim 26 \mu\text{m}$  centres which considerably stabilize the cross section of the channel. However, because any small changes in the gap size between posts will affect the critical diameter in the device it is important to separate these effects, if any,

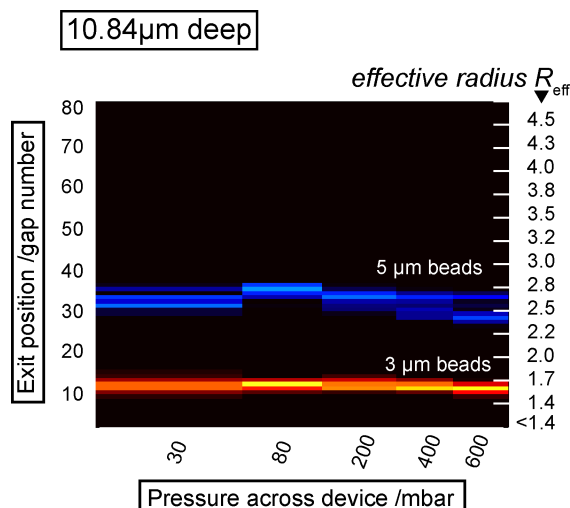


Fig. ESI 6 There is very little systematic change in the outlet distributions of hard polystyrene microspheres as the driving pressure, and consequently the shear-induced stress, is increased.

from the effects of particle deformation. In order to test the effects of device deformation polystyrene microspheres of 3  $\mu\text{m}$  and 5  $\mu\text{m}$  diameters were separated in the device over the pressure range used for the RBC experiments. As can be seen in Fig. ESI 6 there was no systematic change in the effective size of the microspheres and we can neglect both PDMS deformation and hydrodynamic lift in this pressure range in these devices.

1. A. L. Li, H. Seipelt, C. Muller, Y. D. Shi and G. M. Artmann, *Pharmacology & Toxicology*, 1999, **85**, 206-211.
2. B. S. Hardy, K. Uechi, J. Zhen and H. P. Kavehpour, *Lab Chip*, 2009, **9**, 935-938.